

Iterative solvers for image denoising with diffusion models: A comparative study



Subit K. Jain^a, Rajendra K. Ray^{a,*}, Arnav Bhavsar^b

^a School of Basic Sciences, Indian Institute of Technology Mandi, Pin 175001, India

^b School of Computing and Electrical Engineering, Indian Institute of Technology Mandi, Pin 175001, India

ARTICLE INFO

Article history:

Received 13 July 2014

Received in revised form 24 January 2015

Accepted 5 April 2015

Available online 4 May 2015

Keywords:

Perona–Malik

Bilateral filter

Crank–Nicolson scheme

Successive-over-relaxation

Hybrid bi-conjugate gradient stabilized
method

Denoising

ABSTRACT

In this paper we propose and compare the use of two iterative solvers using the Crank–Nicolson finite difference method, to address the task of image denoising via partial differential equations (PDEs) models such as Regularized Perona–Malik equation or C-model and Bazan model (Bilateral-filter-based model). The solvers which are considered in this paper are the Successive-over-Relaxation (SOR) and an advanced solver known as Hybrid Bi-Conjugate Gradient Stabilized (Hybrid BiCGStab) method. From numerical experiments, it is found that the Crank–Nicolson method with hybrid BiCGStab iterative solver produces better results and is more efficient than SOR and already existing, in terms of MSSIM and PSNR.

© 2015 Elsevier Ltd. All rights reserved.

1. Introduction

Image processing plays an important role in medical imaging, remote sensing, military, computer graphics, molecular imaging, surveillance video, auto-piloting, etc. During the past two decades, image processing has attracted the attention of many mathematicians. One of the most fundamental tasks in image processing applications is that of image de-noising, which is a significant preprocessing step. Due to inherent limitations of acquisition devices or the existence of random interruptions in the medium, most images are naturally dissipated by noise. Typically, it is assumed that the degradation process for image denoising can be expressed using a mathematical model [1].

For a long time, partial differential equations (PDEs) are a very effective tool to obtain a denoised image from noisy image [2–4]. The linear diffusion process is the simplest and well considered PDE-based method [5]. But it fails to keep edges or textures in the denoised image as a result of the low-pass convolution [6]. In recent years, the applications of nonlinear PDEs are popular in the field of image restoration to address the image de-noising problem. Numerous nonlinear PDE models are proposed for this purpose [7,8]. In [6], Perona and Malik proposed a nonlinear PDE which consists of an inhomogeneous diffusion coefficient. This model is useful for smoothing, de-noising and detection of edges in (digital) image. However, Perona–Malik (P–M) model is an ill-posed model [9]. Hence to attain a well-posed model Catté et al. [10] proposed a regularization of the P–M model, known as regularized Perona–Malik model, in which they modified this model by convolving image with Gaussian kernel for the diffusion coefficient.

Recently, Tomasi and Manduchi proposed a bilateral filter for removing noise from images, which combines spatial and range filtering [11]. Bilateral filter depends on spatial difference and intensity difference. In bilateral filter, a pixel

* Corresponding author.

E-mail addresses: jain.subit@gmail.com (S.K. Jain), rajendra@iitmandi.ac.in (R.K. Ray), arnav@iitmandi.ac.in (A. Bhavsar).



Fig. 1. Boat noise free image (Top Left), noisy image with $\sigma = 20$ (Top Right), restored image using Existing scheme [10] (Down left), SOR solver based proposed scheme (Down middle) and Hybrid BiCGStab solver based proposed scheme (Down Right).

is simply replaced by weighted mean of its neighbors having similar gray level values and weighting the distance to the reference pixel [12]. It has been adopted for several applications like medical imaging, image restoration, etc. [13,14]. This is a non-iterative technique, but only if size of spatial box is large enough and this cause for over smoothing. Hence to do denoising it should be able to make balance between edge preservation and spatial window size. It is known that anisotropic diffusion plays important role for image denoising. Therefore the combination of anisotropic diffusion and bilateral filter has attracted many researchers in this decade, to improve the quality of denoised or filtered image while preserving the edge information [15–17,13,14,18]. In this work we have adopted the Bazan model.

The above discussed theory related to PDE models is continuous in nature. However, in practical problems, the image is discrete and represented by a collection of pixels on a fixed equidistant grid. Moreover, in most PDE models, analytical solutions are not possible. Thus, the diffusion filter models must be discretized by proper numerical schemes to compute the solutions. The development of selected numerical technique for the PDE models is a vital factor of PDE-based approaches [19]. One popular numerical scheme, in this respect is the Crank–Nicolson scheme [20], which has some advantages over traditional schemes, as discussed in Section 1.1.

In addition to choosing a proper numerical scheme, the iterative approaches, which are used to solve the system of algebraic equations generating from the numerical discretization, are also important considering factors such as faster convergence and better denoising accuracy [21]. A useful solver in this respect which has not yet been explored for image denoising is the Hybrid Bi-Conjugate Gradient Stabilized solver (BiCGStab(2)) [22].

In this paper, our main intention is to study the usefulness of advance iterative solvers (e.g. Hybrid BiCGStab method) for the popular Crank–Nicolson (C–N) Numerical Scheme, for image de-noising, when the model equations are non-linear and discretized using implicit numerical scheme.

1.1. Related work

Till date only few finite difference schemes are available to solve these PDE models. Usually the explicit numerical schemes have been used to discretize the corresponding nonlinear diffusion models [23]. Because the explicit scheme has the limitations of instability and several iterations [23,19,24], an important alternative is to use the implicit numerical scheme e.g. Crank–Nicolson (C–N) or higher order accurate numerical methods, to solve these models to get better denoising accuracy [25,26]. The use of C–N method has advantages such as unconditional stability, second order accuracy in time and space, and its mathematical/computational competency to find the optimal time step size [20].

It is quite cumbersome to solve such systems using direct methods, because of the requirement of memory space and the huge CPU times. Hence, to achieve better accuracy and speed up the calculation, iterative solvers have been used. Again, the accuracy of a numerical method depends on the right choice of iterative solver, which is ultimately going to solve the algebraic system of equations originating from the finite difference discretization. The problem, however, is that it requires a good knowledge and proficiency to select the proper iterative solvers [21,27,28]. The Krylov subspace methods like



Fig. 2. Cameraman noise free image (Top Left), noisy image with $\sigma = 20$ (Top Right), restored image using Existing scheme [10] (Down left), SOR solver based proposed scheme (Down middle) and Hybrid BiCGStab solver based proposed scheme (Down Right).



Fig. 3. Boat noise free image (Top Left), noisy image with $\sigma = 50$ (Top Right), restored image using Existing scheme [10] (Down left), SOR solver based proposed scheme (Down middle) and Hybrid BiCGStab solver based proposed scheme (Down Right).

Conjugate Gradient (CG) [29], Conjugate Gradient Squared (CGS) [30], Bi-Conjugate Gradient (Bi-CG) [31], Bi-CG Stabilized (BiCGStab) [32] and Generalized Minimal Residual (GMRES) [33] are more popular among the iterative solvers to solve nonsymmetrical linear systems.

The conjugate gradient (CG) method is one of the earlier iterative methods developed using Krylov subspace approach and can be employed to solve large sparse systems, which are difficult to taken care by direct methods. This method generates a sequence of conjugate vectors and these vectors are the residuals of the iterations. This method will converge in not more than n iterations where n is the size of coefficient matrix [29]. This method is useful when the coefficient matrix (A)



Fig. 4. Cameraman noise free image (Top Left), noisy image with $\sigma = 50$ (Top Right), restored image using Existing scheme [10] (Down left), SOR solver based proposed scheme (Down middle) and Hybrid BiCGStab solver based proposed scheme (Down Right).

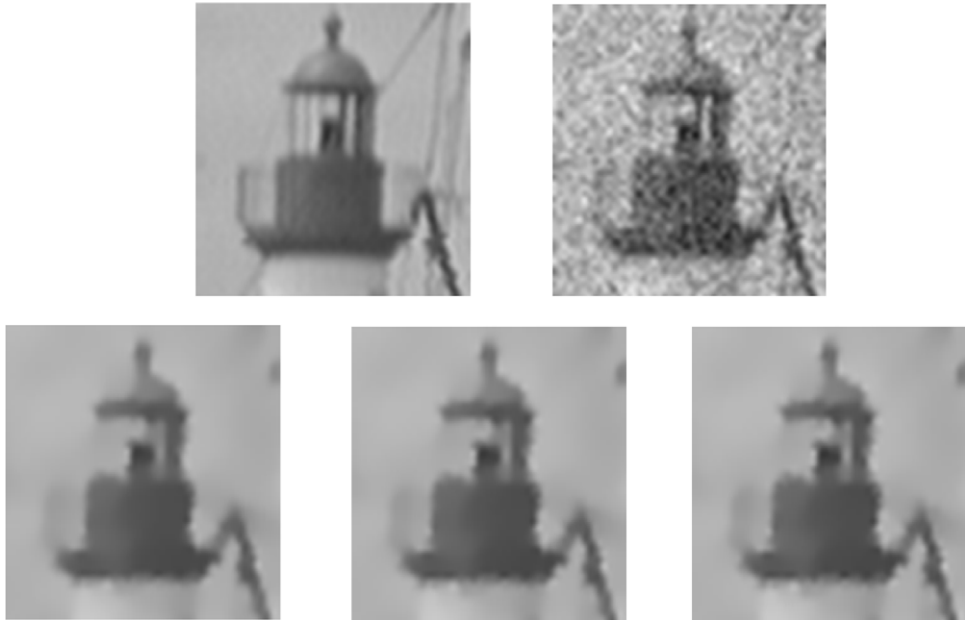


Fig. 5. Sub-image from Boat image. Tower view of Boat noise free image (Top Left), noisy image with $\sigma = 20$ (Top Right), restored image using existing scheme [10] (Down left), SOR solver based proposed scheme (Down middle) and Hybrid BiCGStab solver based proposed scheme (Down Right).

of the algebraic system of equations ($AX = B$) generating from the finite difference discretization is symmetric positive definite. But if the matrix is non-symmetric then an effective alternative is the Bi-CG iterative solver, which is also attractive due to short recursions. However, Bi-CG is not capable to minimize the residual in a suitable norm. On the other hand, the GMRES method mentioned above minimizes the residual over the search space with the shortcoming of long recursions [22]. Hence, to overcome this irregular convergence behavior, hybrid methods have been proposed. In numerical linear algebra, hybrid methods are blend of standard Krylov subspace methods. The Hybrid Biconjugate Gradient Stabilized method, often

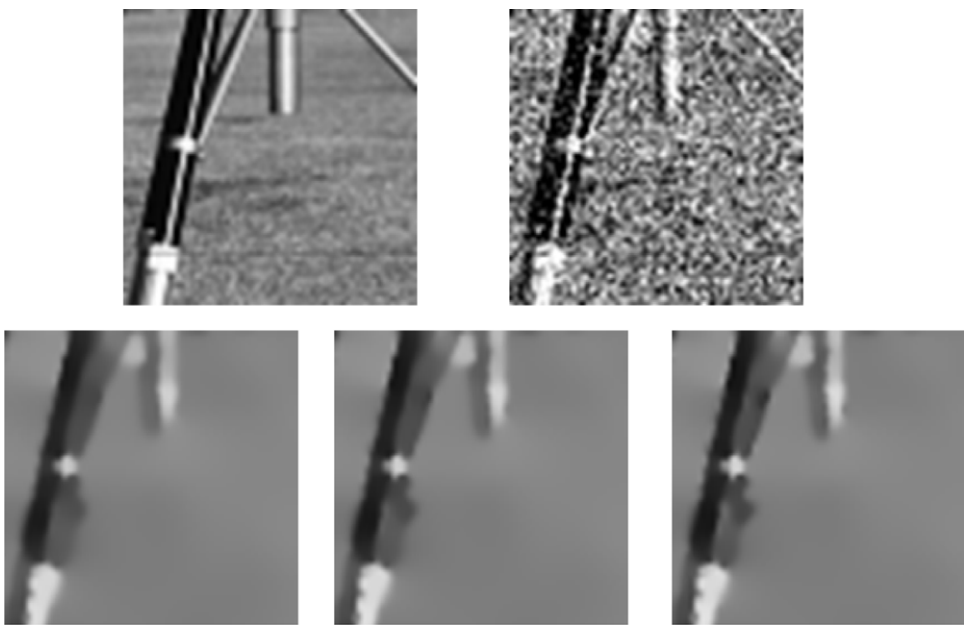


Fig. 6. Sub-image from Cameraman image. Stand view of Cameraman noise free image (Top Left), noisy image with $\sigma = 50$ (Top Right), restored image using Existing scheme [10] (Down left), SOR solver based proposed scheme (Down middle) and Hybrid BiCGStab solver based proposed scheme (Down Right).

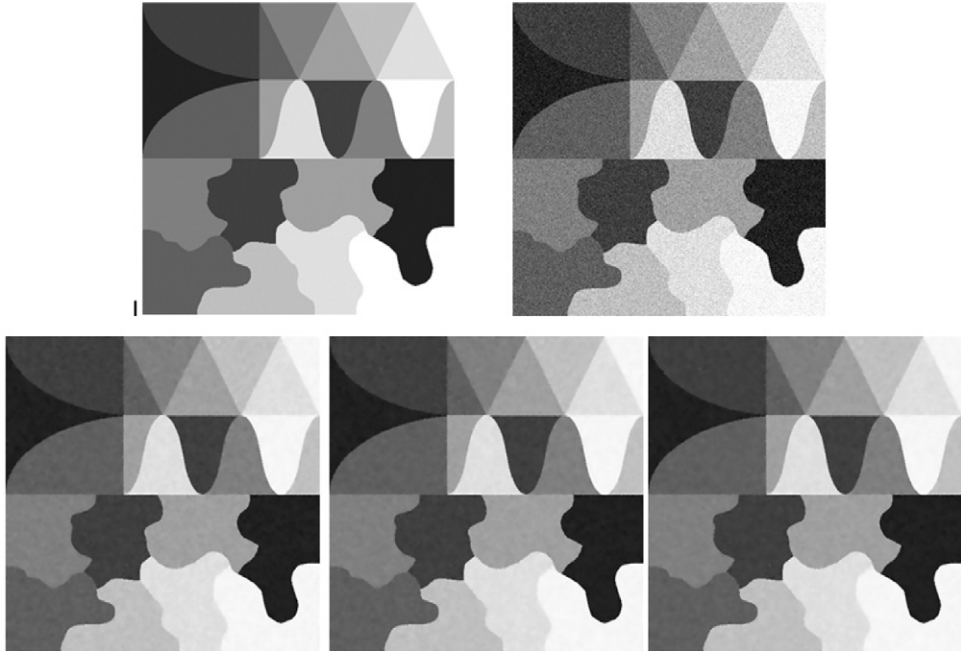


Fig. 7. Texture1 (Synthetic) noise free image (Top Left), noisy image with $\sigma = 20$ (Top Right), restored image using existing scheme [10] (Down left), SOR solver based proposed scheme (Down middle) and Hybrid BiCGStab solver based proposed scheme (Down Right).

abbreviated as Hybrid BiCGStab (or BiCGStab(2)) is one such combination of Bi Conjugate Gradient method and low degree GMRES method. To solve the non-symmetric linear systems numerically, Hybrid BiCGStab is developed by H. A. van der Vorst [22]. It has faster and smoother convergence in comparison to the original Bi-CG and its other variants like CGS, etc.

This work presents the application of the Hybrid BiCGStab solver for the task of image denoising using the finite difference discretization of two models (C-model and Bazan model). We have discretized these models using the C-N scheme. We

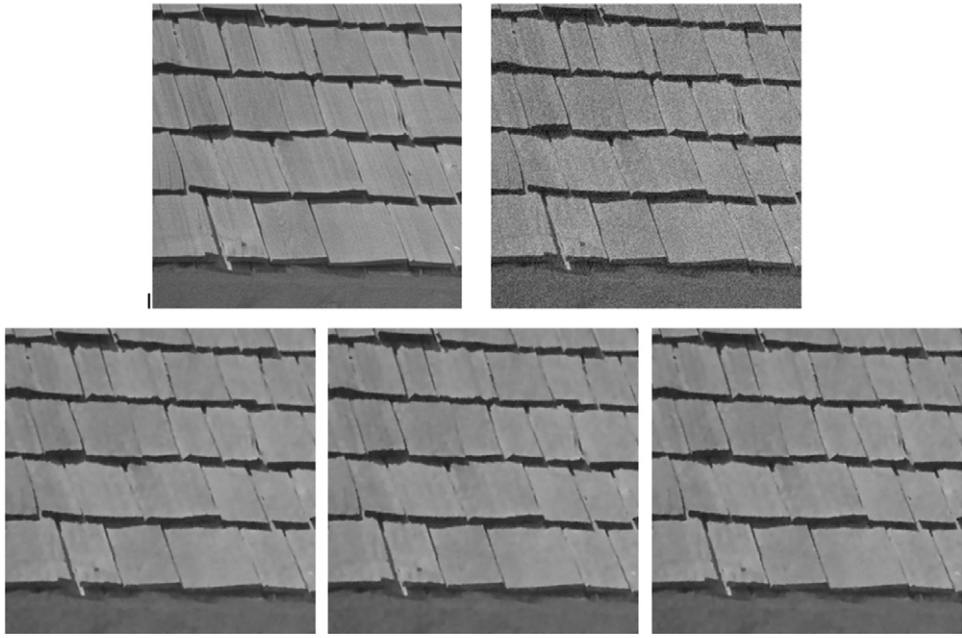


Fig. 8. Texture2 (Real) noise free image (Top Left), noisy image with $\sigma = 20$ (Top Right), restored image using existing scheme [10] (Down left), SOR solver based proposed scheme (Down middle) and Hybrid BiCGStab solver based proposed scheme (Down Right).

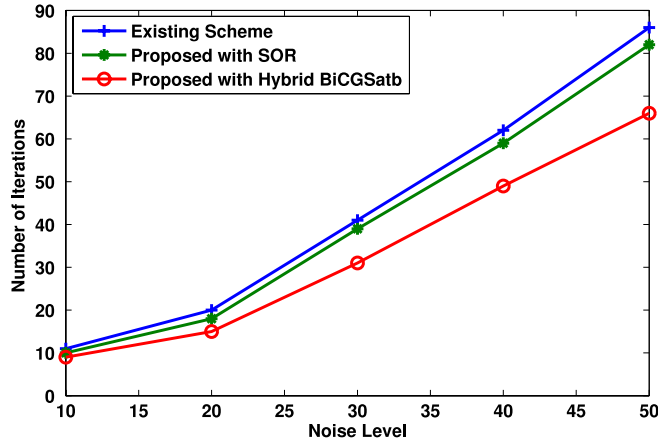


Fig. 9. Noise level v/s number of iterations for Lena image using C-model with existing scheme [10], SOR solver based proposed scheme and Hybrid BiCGStab solver based proposed scheme.

compare the results of Hybrid BiCGStab solver with another existing iterative solver viz. SOR, which nothing but the weighted average of the previous iterates output and the computed Gauss-Seidel iterate successively for each component and also weight is chosen as, it will speed up the convergence rate of the iterates to the solution [21] and also with the results obtained by existing methods [10,15]. In addition to better denoising performance (in terms of quantitative metrics), we also demonstrate a much higher efficiency of the proposed denoising strategy. To the best of our knowledge, this type of study in the field of image de-noising has not been done yet.

The paper is organized as follows. In Section 2 we have given concise survey on related PDE models. Our numerical scheme is given in Section 3. A brief discussion on iterative solvers has been presented in Section 4. In Section 5 we evaluate the experimental results by applying the C-N scheme and two iterative solvers. We conclude the proposed work with summary in Section 6.



Fig. 10. Boat noise free image (Top Left), noisy image with $\sigma = 40$ (Top Right), restored image using Existing scheme [10] (Down left), SOR solver based proposed scheme (Down middle) and Hybrid BiCGStab solver based proposed scheme (Down Right) for 40 iterations.

2. Related PDE-models

2.1. Regularized Perona–Malik or C-model

Perona and Malik [6] proposed the general divergence diffusion form for scale space description of images and edge detection. They replaced the linear isotropic diffusion equation with a nonlinear PDE, which has the form,

$$\left\{ \begin{array}{ll} I_t = \nabla(c(|\nabla I|^2)\nabla I) & \text{in } \Omega \times (0, +\infty) \\ \frac{\partial I}{\partial n} = 0 & \text{in } \partial\Omega \times (0, +\infty) \\ I(x, y, 0) = I_0(x, y) & \text{in } \Omega \end{array} \right\} \quad (1)$$

Here Ω is the picture domain, I_0 is the observed image, I is the original image to be recovered, n is the unit normal to the boundary of Ω and $c(s^2)$ is the diffusion coefficient which diffuses the image, while the boundaries of image are preserved. The diffusion coefficient is designed in such a way that its value is small for inhomogeneous region i.e. the diffusion is low and its value is high for homogeneous region i.e. diffusion is tending to smoothness. The diffusion coefficient has some properties as $c(0) = 1$, $c(s^2) \rightarrow 0$ as $s \rightarrow \infty$.

While the P–M model performs well in practice, it is mathematically ill-posed. This is the so-called Perona–Malik paradox [9]. It had several serious theoretical and practical difficulties. For these difficulties many people have been attempted to study the P–M equation. In 1992, Catté et al. [10] proposed a PDE, which is known as the Regularized P–M model. This leads to the following model,

$$\left\{ \begin{array}{ll} I_t = \nabla(c(|\nabla I_\sigma|^2)\nabla I) & \text{in } \Omega \times (0, +\infty) \\ \frac{\partial I}{\partial n} = 0 & \text{in } \partial\Omega \times (0, +\infty) \\ I(x, y, 0) = I_0(x, y) & \text{in } \Omega \end{array} \right\}. \quad (2)$$

With $I_\sigma = G_\sigma * I$: I_σ is the smoothed version of image I convolved by a Gaussian smoothing kernel G_σ . For the convenience, we call this equation as C-equation or C-model. Catté et al. proved the existence, uniqueness and regularity of a solution [10]. This regularization belongs to spatial regularization. Here we adopt the diffusion coefficient as:

$$c(s^2) = \frac{1}{1 + \frac{s^2}{\lambda^2}} \quad (3)$$

here λ is a contrast parameter and a positive constant.

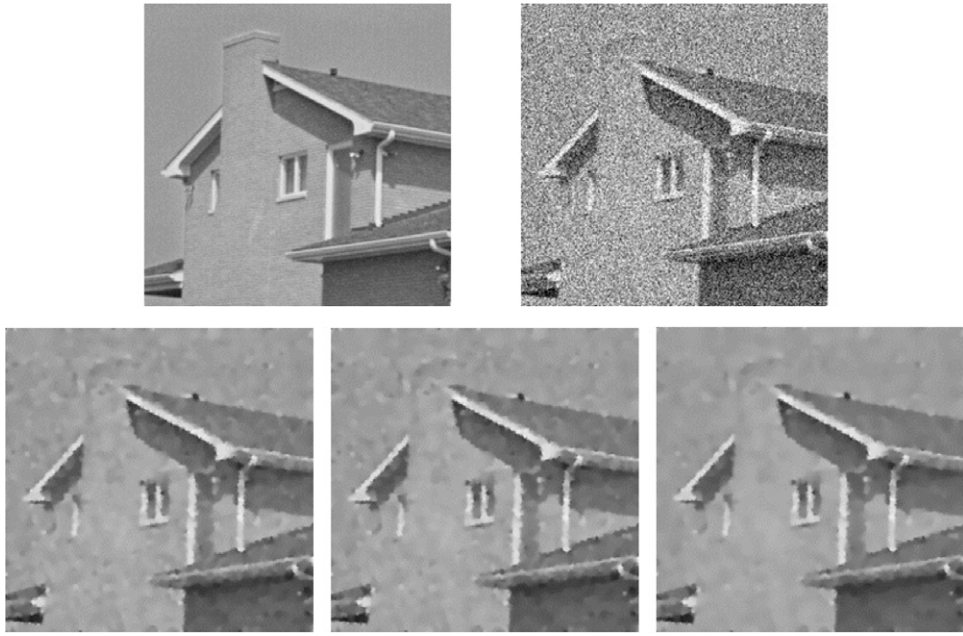


Fig. 11. House noise free image (Top Left), noisy image with $\sigma = 40$ (Top Right), restored image using Existing scheme [10] (Down left), SOR solver based proposed scheme (Down middle) and Hybrid BiCGStab solver based proposed scheme (Down Right) for 40 iterations.

2.2. Bazan model

To combine domain and range filtering with nonlinear diffusion, in 2007, Bazan et al. [15] proposed a combination of nonlinear diffusion and bilateral filtering, in which they replaced the Gaussian smoothed image by bilateral filtered image for diffusion coefficient. The model can be expressed as

$$\begin{cases} I_t = \nabla(c(|\nabla I_{BF}|^2)\nabla I) & \text{in } \Omega \times (0, +\infty) \\ \frac{\partial I}{\partial n} = 0 & \text{in } \partial\Omega \times (0, +\infty) \\ I(x, y, 0) = I_0(x, y) & \text{in } \Omega \end{cases} \quad (4)$$

where

$$I_{BF} = BF(I_p) = \frac{\sum_{q \in S} G_{\sigma_s}(\|p - q\|)G_{\sigma_r}(|I_p - I_q|)I_q}{\sum_{q \in S} G_{\sigma_s}(\|p - q\|)G_{\sigma_r}(|I_p - I_q|)}$$

S is a spatial neighborhood of pixel p . The parameters σ_s and σ_r define the amount of filtering to filter a pixel of an image I . Here diffusivity function is calculated in the same way as Eq. (3).

3. Numerical scheme

This section presents many aspects related to the numerical implementation of Eqs. (2) and (4). To reduce the noise from a noisy image, we have applied the Crank–Nicolson Finite Difference method to solve both the above discussed models. The C–N method is combination of the forward Euler method at n th step and the backward Euler method at $(n + 1)$ th step. The main idea of this method is based on the trapezoidal rule. Hence, our difference scheme is as follows.

Let h represents the spatial step size and τ be the time step. Denote $\hat{I}_{i,j}^n = \hat{I}(x_i, y_j, t_n)$ where $x_i = ih$, $y_j = jh$ and $t_n = n\tau$. Since the diffusion term is approximated by central differences, we use the following notations,

$$\begin{aligned} \frac{\partial I}{\partial x} &= \frac{\hat{I}_{i+1,j}^n - \hat{I}_{i-1,j}^n}{2h}, & \frac{\partial I}{\partial y} &= \frac{\hat{I}_{i,j+1}^n - \hat{I}_{i,j-1}^n}{2h}, \\ \frac{\partial^2 I}{\partial x^2} &= \frac{\hat{I}_{i+1,j}^n - 2\hat{I}_{i,j}^n + \hat{I}_{i-1,j}^n}{h^2}, & \frac{\partial^2 I}{\partial y^2} &= \frac{\hat{I}_{i,j+1}^n - 2\hat{I}_{i,j}^n + \hat{I}_{i,j-1}^n}{h^2}. \end{aligned}$$

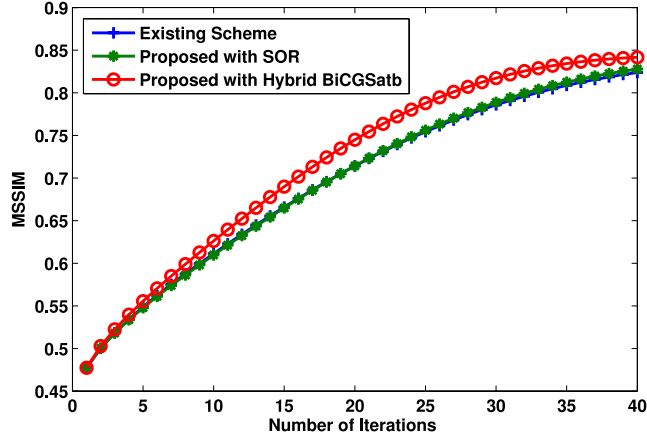


Fig. 12. MSSIM v/s number of iterations for Boat Image with $\sigma = 40$ using existing scheme [10], SOR solver based proposed scheme and Hybrid BiCGStab solver based proposed scheme.

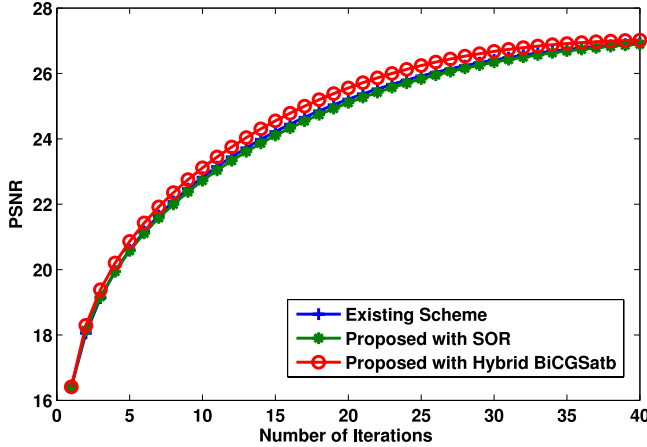


Fig. 13. PSNR v/s number of iterations for Boat Image with $\sigma = 40$ using existing scheme [10], SOR solver based proposed scheme and Hybrid BiCGStab solver based proposed scheme.

Then,

$$\begin{aligned}\nabla(c(|\nabla \hat{I}_{BF}|^2) \nabla \hat{I})|_{i,j}^n &= (C_N \cdot \nabla_N \hat{I} + C_S \cdot \nabla_S \hat{I} + C_W \cdot \nabla_W \hat{I} + C_E \cdot \nabla_E \hat{I})|_{i,j}^n \\ \nabla(c(|\nabla \hat{I}_{BF}|^2) \nabla \hat{I})|_{i,j}^{n+1} &= (C_N \cdot \nabla_N \hat{I} + C_S \cdot \nabla_S \hat{I} + C_W \cdot \nabla_W \hat{I} + C_E \cdot \nabla_E \hat{I})|_{i,j}^{n+1}.\end{aligned}$$

Our scheme is simply

$$\hat{I}_{i,j}^{n+1} = \hat{I}_{i,j}^n + \tau \left(\frac{\nabla(c(|\nabla \hat{I}_{BF}|^2) \nabla \hat{I})|_{i,j}^n + \nabla(c(|\nabla \hat{I}_{BF}|^2) \nabla \hat{I})|_{i,j}^{n+1}}{2} \right).$$

For notations, see [6]. There are large number of unknowns in each system and the sparsity of the coefficient matrix suggests the use of an iterative solver.

4. Iterative solvers

In this section, we focus on the iterative methods. Nowadays in the iterative methods, basic iterative solvers e.g. Jacobi, Gauss-Seidel methods are frequently used for image denoising. These methods are easy to understand but the convergence is slow, moreover these methods are not able to solve all the linear systems [21]. Whereas the Krylov subspace methods are quite complex to understand but it has the faster convergence [34]. The basic idea of the Krylov subspace method is to search for a good approximate solution of linear system from the subspace $\text{span}(b, Ab, A^2b, \dots, A^{k-1}b)$, at iteration k .



Fig. 14. Lena noise free image (Top Left), noisy image with $\sigma^* = 0.01$ (Top Right), restored image using Existing scheme [15] (Down left), SOR solver based proposed scheme (Down middle) and Hybrid BiCGStab solver based proposed scheme (Down Right).

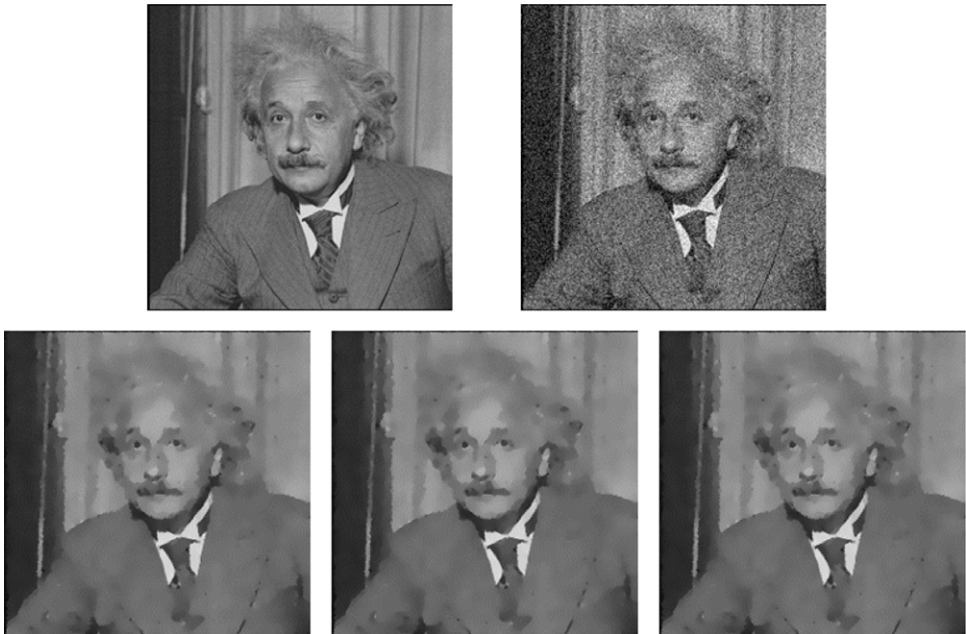


Fig. 15. Einstein noise free image (Top Left), noisy image with $\sigma^* = 0.01$ (Top Right), restored image using existing scheme [15] (Down left), SOR solver based proposed scheme (Down middle) and Hybrid BiCGStab solver based proposed scheme (Down Right).

Hence, as discussed above, to solve the algebraic system of equations arising from the Crank–Nicolson finite difference discretization, we have chosen the SOR and the Hybrid BiCGStab method.

4.1. SOR method

The Successive-over-Relaxation (SOR) method is a kind of relaxation methods. This method is a generalized or improved form of the Gauss–Seidel (GS) method and formed by adding a relaxation parameter. When the solution at k th iteration is



Fig. 16. Lena noise free image (Top Left), noisy image with $\sigma^* = 0.02$ (Top Right), restored image using Existing scheme [15] (Down left), SOR solver based proposed scheme (Down middle) and Hybrid BiCGStab solver based proposed scheme (Down Right).

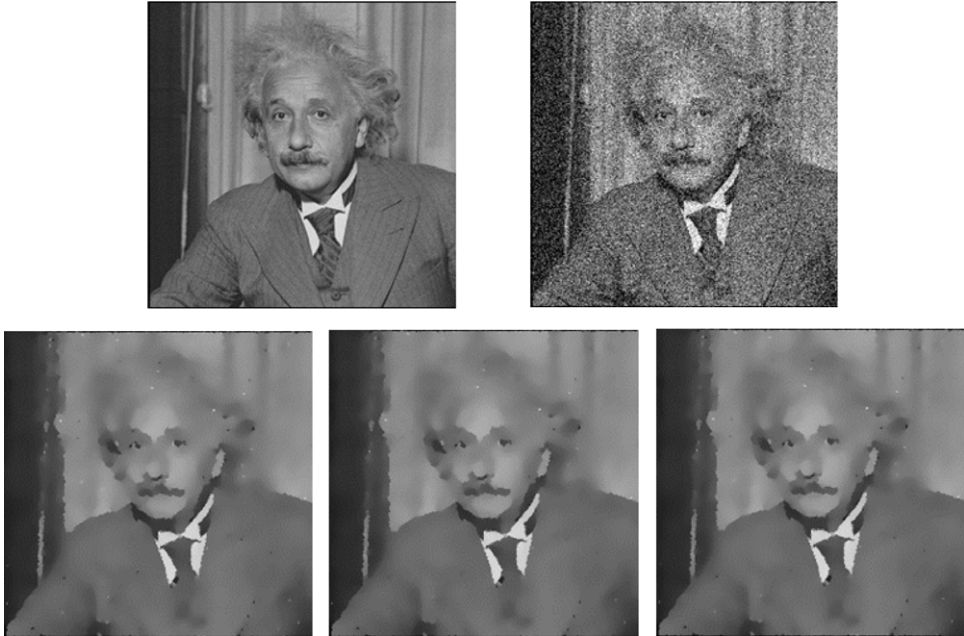


Fig. 17. Einstein noise free image (Top Left), noisy image with $\sigma^* = 0.02$ (Top Right), restored image using existing scheme [15] (Down left), SOR solver based proposed scheme (Down middle) and Hybrid BiCGStab solver based proposed scheme (Down Right).

known then we can calculate the solution at $(k + 1)$ th iteration by applying the SOR method as follows

$$\hat{l}^{k+1} = \omega \bar{l}^{k+1} + (1 - \omega) \hat{l}^k.$$

Here, \bar{l}^{k+1} is the GS solution at $(k + 1)$ th iteration and ω is the relaxation parameter, which is chosen in such a manner that it will accelerate the convergence of the method towards the solution.

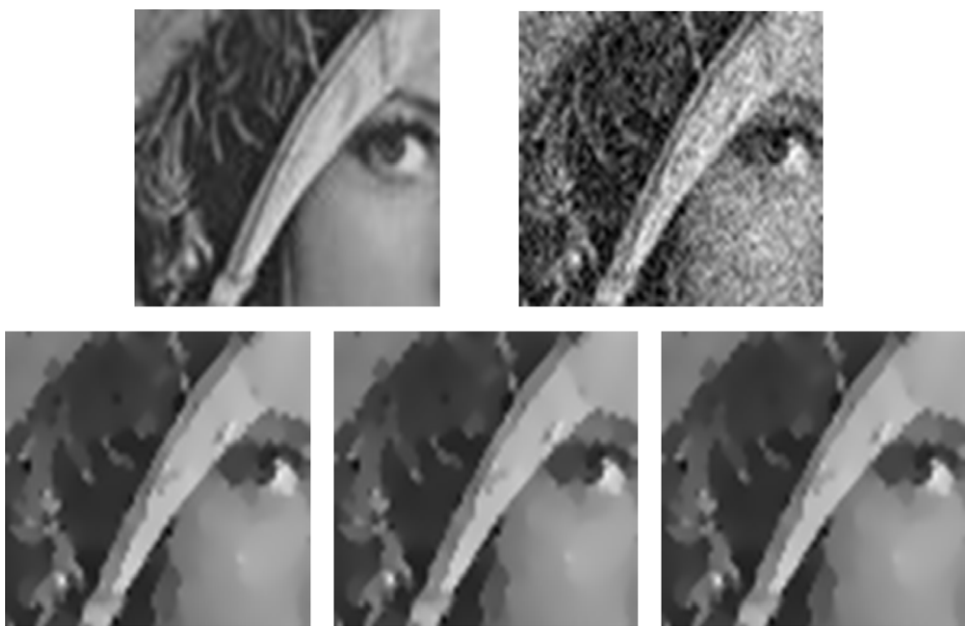


Fig. 18. Sub-image from Lena image. Hat view of Lena noise free image (Top Left), noisy image with $\sigma^* = 0.01$ (Top Right), restored image using existing scheme [15] (Down left), SOR solver based proposed scheme (Down middle) and Hybrid BiCGStab solver based proposed scheme (Down Right).

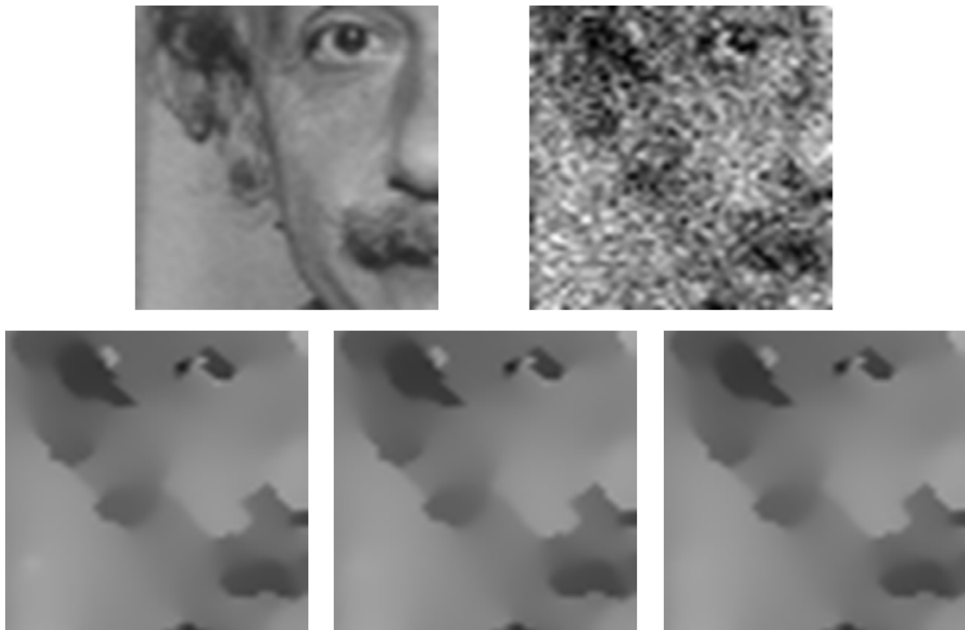


Fig. 19. Sub-image from Einstein image. Eye view of Einstein noise free image (Top Left), noisy image with $\sigma^* = 0.02$ (Top Right), restored image existing scheme [15] (Down left), SOR solver based proposed scheme (Down middle) and Hybrid BiCGStab solver based proposed scheme (Down Right).

4.2. Hybrid BiCGStab method

Hybrid Bi-Conjugate Gradient stabilized method [22] is the combination of Krylov subspace methods in which two steps (even and odd) for Bi-CG and one step for low degree GMRES are performed to solve the system of equations. The algorithm of Hybrid BiCGStab to solve the system

$$\hat{A}\hat{b} = b$$

where $A \in \mathbf{R}^{NXN}$ and $\hat{b}, b \in \mathbf{R}^N$, can be given as in algorithm 1 [22].

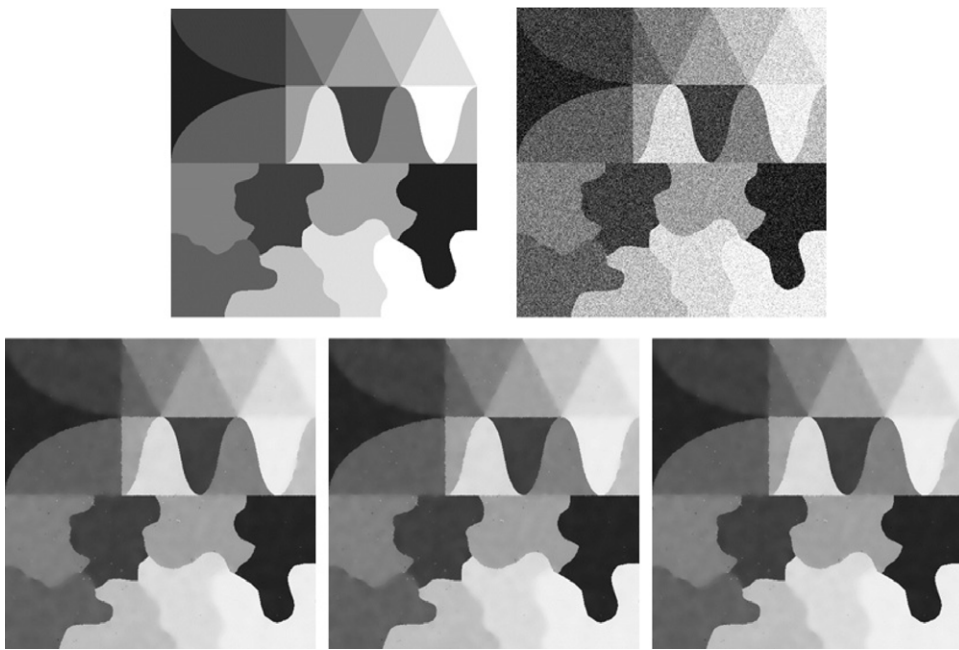


Fig. 20. Texture1 (Synthetic) noise free image (Top Left), noisy image with $\sigma^* = 0.025$ (Top Right), restored image using existing scheme [15] (Down left), SOR solver based proposed scheme (Down middle) and Hybrid BiCGStab solver based proposed scheme (Down Right).

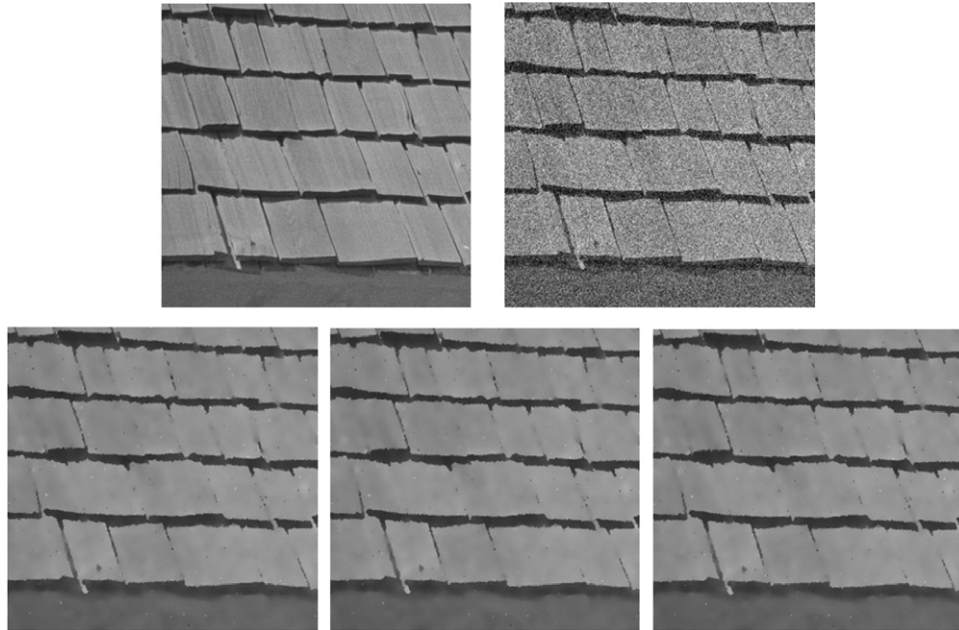


Fig. 21. Texture2 (Real) noise free image (Top Left), noisy image with $\sigma^* = 0.025$ (Top Right), restored image using existing scheme [15] (Down left), SOR solver based proposed scheme (Down middle) and Hybrid BiCGStab solver based proposed scheme (Down Right).

In the algorithm 1, (\cdot, \cdot) is the inner product. As given in algorithm 1, this method has the combined effect of Bi-CG and GMRES(2). The main idea is that after applying 2 successive Bi-CG steps, it is relatively easy to minimize the residual over that particular Krylov subspace. As a result, the Hybrid BiCGStab method leads only to significant residuals in the even-numbered steps and the odd-numbered steps do not lead necessarily to useful approximations. This method takes less computational memory due to requirement of less number of vector updates, inner-products and vector multiplication for full cycle. Also in the case of break-down, the Hybrid BiCGStab method works better than BICGSTAB or its other variants.

Table 1
PSNR and MSSIM of the test images for C-Model with existing [10] and proposed strategy.

Images	Measure	$\sigma = 10$		$\sigma = 20$		$\sigma = 30$		$\sigma = 40$		$\sigma = 50$	
		Existing scheme [10]	Proposed with SOR								
Lena	MSSIM	0.9163	0.9164	0.9168	0.8576	0.8589	0.8113	0.8148	0.7843	0.7858	0.7868
	PSNR	32.86	32.88	32.88	29.63	29.63	29.62	27.93	27.91	26.94	26.94
Coin	MSSIM	0.8749	0.8829	0.8869	0.8465	0.8523	0.8295	0.8347	0.8400	0.8229	0.8285
	PSNR	29.26	29.67	29.88	27.88	28.12	28.28	26.86	27.07	27.25	26.19
Barb	MSSIM	0.8485	0.8514	0.8529	0.7855	0.7864	0.7397	0.7406	0.7045	0.7055	0.7062
	PSNR	29.31	29.41	29.46	27.08	27.08	27.08	25.82	25.82	24.97	24.97
House	MSSIM	0.8391	0.8398	0.8401	0.7982	0.7991	0.7998	0.7734	0.7720	0.7547	0.7561
	PSNR	33.61	33.61	33.61	31.32	31.32	31.31	29.93	29.93	28.85	28.85
Boat	MSSIM	0.9582	0.9589	0.9596	0.9025	0.9084	0.9124	0.8559	0.8620	0.8666	0.8247
	PSNR	32.84	32.97	32.96	29.35	29.67	29.67	27.68	27.85	27.96	26.62
Camerman	MSSIM	0.8816	0.8844	0.8843	0.8214	0.8247	0.8273	0.7759	0.7812	0.7253	0.7327
	PSNR	31.14	31.33	31.31	27.96	28.11	28.19	26.02	26.12	26.20	24.21
Texture1	MSSIM	0.9785	0.9801	0.9815	0.9641	0.9680	0.9699	0.9602	0.9633	0.9653	0.9549
	PSNR	39.60	39.70	39.79	35.11	35.23	35.30	32.41	32.49	32.54	30.22
Texture2	MSSIM	0.8965	0.8975	0.8983	0.8482	0.8505	0.8527	0.8093	0.8119	0.8145	0.7852
	PSNR	29.43	29.45	29.48	28.17	28.21	28.24	27.28	27.34	27.38	26.68

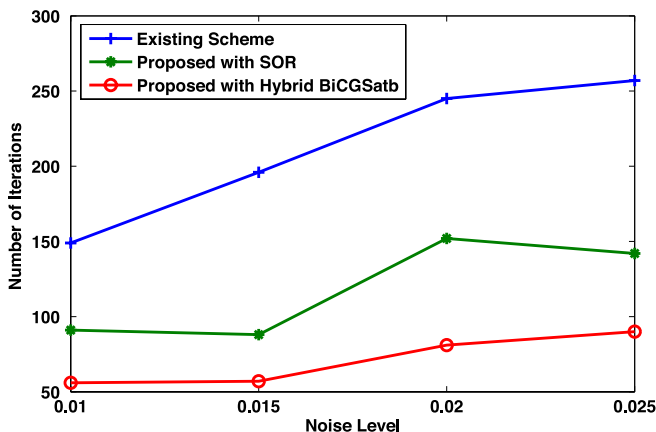


Fig. 22. Noise level v/s number of iterations for Einstein image using Bazan model with existing scheme [15], SOR solver based proposed scheme and Hybrid BiCGStab solver based proposed scheme.



Fig. 23. Lena noise free image (Top Left), noisy image with $\sigma = 0.01$ (Top Right), restored image using existing scheme [15] (Down left), SOR solver based proposed scheme (Down middle) and Hybrid BiCGStab solver based proposed scheme (Down Right) for 40 iterations.

Table 2
Processing time and number of iterations for the C-model.

Images	Measure	$\sigma = 20$		
		Existing scheme [10]	Proposed with SOR	Proposed with Hybrid BiCGStab
Lena	Time (s)	41.1215	51.4860	33.0932
	Iterations	20	18	15
Barb	Time (s)	30.1629	39.5618	25.4477
	Iterations	19	18	15
House	Time (s)	45.4269	59.8967	39.6609
	Iterations	22	21	17
Cameraman	Time (s)	39.9659	49.3682	33.9534
	Iterations	19	17	14

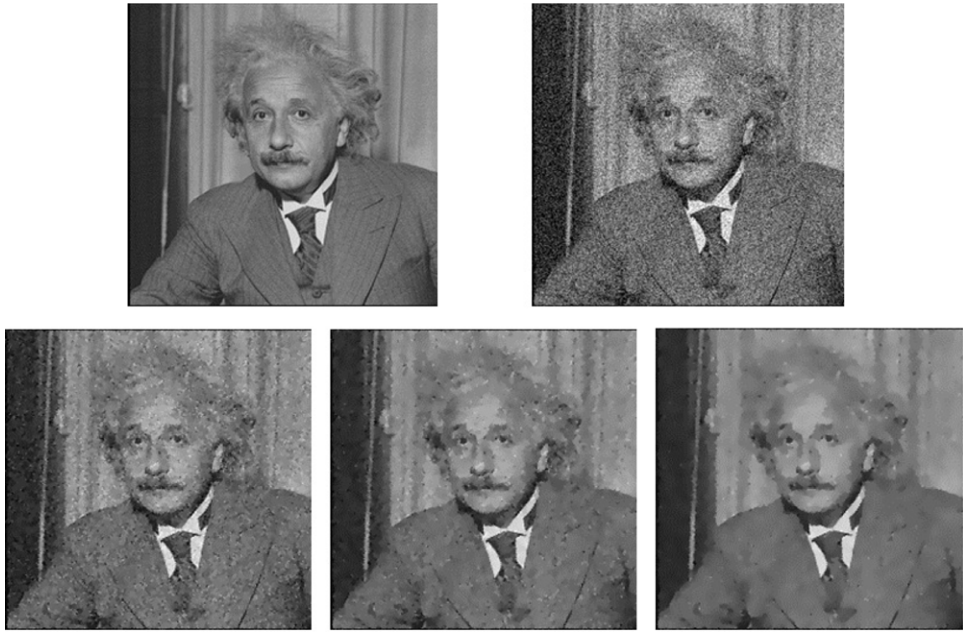


Fig. 24. Einstein noise free image (Top Left), noisy image with $\sigma^* = 0.01$ (Top Right), restored image using existing scheme [15] (Down left), SOR solver based proposed scheme (Down middle) and Hybrid BiCGStab solver based proposed scheme (Down Right) for 40 iterations.

Table 3
MSSIM and PSNR for fixed number of iterations for C-model.

Images	Measure	$\sigma = 40$ (40 iterations)			$\sigma = 50$ (60 iterations)		
		Existing scheme [10]	Proposed with SOR	Proposed with Hybrid BiCGStab	Existing scheme [10]	Proposed with SOR	Proposed with Hybrid BiCGStab
Lena	MSSIM	0.7771	0.7786	0.7881	0.7520	0.7527	0.7595
	PSNR	26.78	26.73	26.89	25.93	25.89	25.99
Cameraman	MSSIM	0.7330	0.7372	0.7490	0.7085	0.7114	0.7188
	PSNR	24.94	24.98	25.02	23.95	23.99	23.98
House	MSSIM	0.7318	0.7342	0.7515	0.7209	0.7226	0.7350
	PSNR	28.32	28.30	28.68	27.67	27.66	27.95
Boat	MSSIM	0.8239	0.8279	0.8417	0.7991	0.8026	0.8146
	PSNR	26.92	26.89	27.02	26.06	26.05	26.11

5. Experimental results

In this section we evaluate the proposed scheme and compare its results with those of the results obtained by the C-model and the Bazan model. We use a stopping criterion proposed in [35] for our scheme. Apart from this, some other approaches have also been proposed for defining the stopping criteria [36–42]. In the MN method [35], the stopping time for diffusion process is chosen in such a way that the correlation between the restored image and noise is minimized and can be expressed as,

$$T = \arg \min_t \text{corr}(I(0) - \hat{I}(t), \hat{I}(t))$$

where

$$\text{corr}(I(0) - \hat{I}(t), \hat{I}(t)) = \frac{\text{cov}(I(0) - \hat{I}(t), \hat{I}(t))}{(\text{var}(I(0) - \hat{I}(t)) \cdot \text{var}(\hat{I}(t)))^{1/2}}.$$

Here $I(0)$ and $\hat{I}(t)$ are the initial and restored images. This criterion finds more applications, as it is based on the idea that the signal in the input image and the noise is uncorrelated. The MN method requires no prior knowledge of the noise statistics. For experiments, we used the set of standard test images of size 256×256 . Images are degraded with white Gaussian noise of zero mean and different level of standard deviations.

Algorithm 1 Algorithm of Hybrid BiCGStab Method for Image Denoising

```

1: Inputs:  $x_0$  as initial solution or initial noisy image,
   matrix  $A$  and vector  $b$ .
2: Calculate residual vector  $r_0 = b - Ax_0$ 
   Set  $r_0$  as an arbitrary vector such that  $r_0 = r = r_0$ 
   Initialize  $\rho_1 = \alpha = \omega_1 = \omega_2 = 1$  and  $w = v = p = 0$ 
3: For  $i = 0, 2, 4, \dots$  till convergence do
4: Calculate  $\rho_0 = -\omega_2\rho_1$ 
   Even BiCG Steps
5: Calculate  $\rho_1 = (r_i, \hat{r}_0)$ ;  $\beta = \frac{\alpha\rho_1}{\rho_0}$ ;
   Set  $\rho_0 = \rho_1$ ;
6: Calculate  $p = r_i - \beta(p - \omega_1v - \omega_2w)$ ;
7:  $v = Ap$ ;
8:  $\gamma = (v, \hat{r}_0)$ ;  $\alpha = \frac{\rho_0}{\gamma}$ ;
9:  $r = r_i - \alpha v$ ;
10:  $s = Ar$ ;
11:  $x = x_i + \alpha p$ ;
   Odd BiCG Steps
12: Calculate  $\rho_1 = (s, \hat{r}_0)$ ;  $\beta = \frac{\alpha\rho_1}{\rho_0}$ ;
   Set  $\rho_0 = \rho_1$ ;
13:  $v = s - \beta v$ ;
14:  $w = Av$ ;
15:  $\gamma = (w, \hat{r}_0)$ ;  $\alpha = \frac{\rho_0}{\gamma}$ ;
16:  $p = r - \beta p$ ;
17:  $r = r - \alpha v$ ;
18:  $s = s - \alpha w$ ;
19:  $t = As$ ;
   GMRES(2)
20:  $\omega_1 = (r, s)$ ;  $\omega_2 = (r, t)$ ;  $\mu = (s, s)$ ;  $\tau = (t, t)$ ;  $v = (s, t)$ ;
21:  $\tau = \tau - \frac{v^2}{\mu}$ 
22:  $\omega_2 = \frac{\omega_2 - \frac{v\omega_1}{\mu}}{\tau}$ 
23:  $\omega_1 = \frac{\omega_1 - v\omega_2}{\mu}$ 
24:  $x_{i+2} = x + \alpha p + \omega_1 r + \omega_2 s$ ;
25:  $r_{i+2} = r - \omega_1 s - \omega_2 t$ ;
26: end

```

For all noisy and denoised images, MSSIM [43] and PSNR [44] are calculated so as to make efficient comparisons between considered iterative solvers. The formula used for calculating PSNR and SSIM is as follows

$$\text{SSIM}(x, y) = \frac{(2\mu_x\mu_y + c_1)(2\sigma_{xy} + c_2)}{(\mu_x^2 + \mu_y^2 + c_1)(\sigma_x^2 + \sigma_y^2 + c_2)}$$

$$\text{PSNR} = 10 \log_{10} \left(\frac{\max(I_0)^2}{\frac{1}{rc} \sum_{i=1}^r \sum_{j=1}^c (I_t - I_0)^2} \right).$$

Here $\mu_x, \mu_y, \sigma_x^2, \sigma_y^2, \sigma_{xy}$ are the average, variance and covariance of x and y , respectively. c_1 and c_2 are the variables to stabilize the division with weak denominator. For both quality measures, a high value suggests that the filtered image is closer to the noise free image.

The results using existing Catté's scheme [10] and proposed denoising strategy for the C-model are shown in various standard test images in Figs. 1–8. Figs. 1–6 show the results for natural images whereas Figs. 7 and 8 show same results for typical textured images. We have tested our approaches for different noise standard deviations e.g. $\sigma \in (10, 50)$ and report quantitative measures for the same. In all cases we compare the denoising results of existing Catté's scheme, proposed method with SOR and proposed method with Hybrid BiCGStab. Our denoising results are better than the existing Catté's scheme in PSNR, MSSIM and visual quality. For our proposed strategy, the denoising performance of using Hybrid BiCGStab method is better than using the SOR method. For these results all the approaches were run till the stopping criterion is met. From these figures, we can observe that the Hybrid BiCGStab method is more capable to restore or preserve the contrast at edges in comparison to SOR and existing Catté's approach, while also removing the noise effectively.

The results of the image quality measures are shown in Table 1 in terms of PSNR and MSSIM. This clearly indicates that the Hybrid BiCGStab method is more capable of dealing with noise than SOR as shown by higher values of PSNR and MSSIM, which show that the proposed denoising strategy is robust in improving the denoising capability of the discussed method.

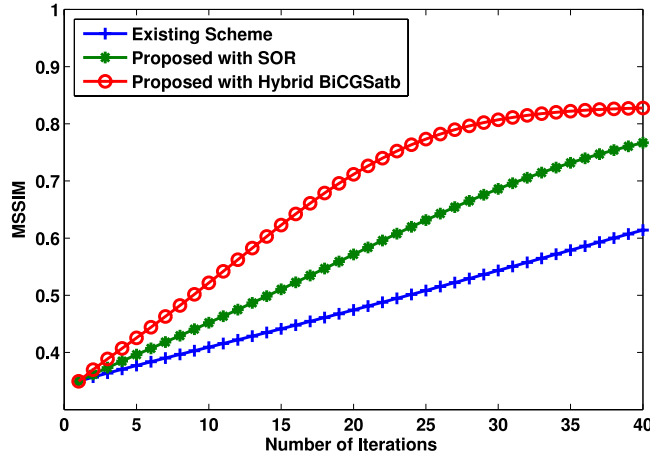


Fig. 25. MSSIM v/s number of iterations for Lena Image with $\sigma_* = 0.01$ using existing scheme [15], SOR solver based proposed scheme and Hybrid BiCGStab solver based proposed scheme.

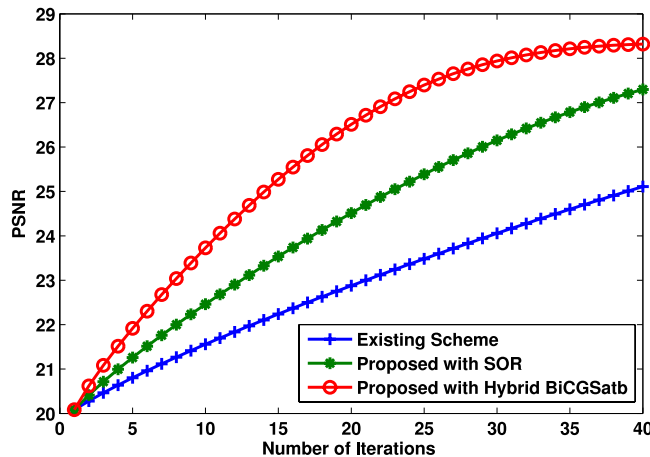


Fig. 26. PSNR v/s number of iterations for Lena Image with $\sigma_* = 0.01$ using existing scheme [15], SOR solver based proposed scheme and Hybrid BiCGStab solver based proposed scheme.

Moreover, when the image suffers from a higher noise standard deviation, the Hybrid BiCGStab method can improve the PSNR and MSSIM values larger than that of the lower noise standard deviation case.

In addition to improved denoising, from Table 2 and Fig. 9 we can observe that the proposed algorithm satisfies the stopping criteria in the much lesser iterations as well as less computational time. Hence, from above we may conclude that the proposed strategy is much more efficient than the existing approaches for denoising for the C-model.

To reinforce the argument about denoising quality and efficiency, we show in Figs. 10–11 the denoising for a fixed number of iterations across all the methods. The proposed method greatly outperforms the others, in this respect. Figs. 12–13 depict the performance of the proposed method in terms of MSSIM and PSNR values respectively. This is also verified quantitatively in Table 3.

We then compare the performance of both solvers to denoise images, which are degraded with white Gaussian noise of zero mean and different standard deviations e.g. $\sigma_* \in (0.01, 0.025)$, using the Bazan model. We make comparisons with the Bazan model. In this work, the author used the σ value in the normalized intensity range. Hence, to make the efficient comparison, images are normalized in the range $[0, 1]$ and then noise is added and shown as σ_* . The filtered images denoised using Bazan model with different numerical strategies are shown in Figs. 14–21. Figs. 14–19 show the results for natural images whereas Figs. 20 and 21 show same results for typical textured images. Table 4 shows the quantitative results for the same parameters as considered in Table 1, for the Bazan model.

From quantitative results for Bazan model, higher values of PSNR and MSSIM clearly depicted that the proposed denoising strategy works better for this denoising model also. Again, from Table 5 and Fig. 22 we can easily find that the Hybrid BiCGStab iterative solver with Bazan model takes less iteration numbers and computational time to converge. Again, similar

Table 4
PSNR and MSSIM of the test images for Bazan Model with existing [15] and proposed strategies.

Images	Measure	$\sigma^* = 0.01$		$\sigma^* = 0.015$		$\sigma^* = 0.02$		$\sigma^* = 0.025$	
		Existing scheme [15]	Proposed with SOR	Proposed with Hybrid BiCGSatb	Existing scheme [15]	Proposed with SOR	Proposed with Hybrid BiCGSatb	Existing scheme [15]	Proposed with SOR
Lena	MSSIM	0.8272	0.8275	0.8277	0.7972	0.7966	0.7972	0.7702	0.7711
	PSNR	28.30	28.32	28.32	27.28	27.27	27.28	26.43	26.46
Barb	MSSIM	0.7486	0.7480	0.7487	0.7154	0.7162	0.7162	0.6835	0.6846
	PSNR	25.96	25.96	25.97	25.16	25.19	25.19	24.48	24.51
Cameraman	MSSIM	0.8036	0.8023	0.8037	0.7756	0.7751	0.7754	0.7579	0.7589
	PSNR	27.24	27.18	27.23	26.17	26.14	26.16	25.57	25.60
Einstein	MSSIM	0.7026	0.7021	0.7034	0.6740	0.6741	0.6752	0.6463	0.6469
	PSNR	28.48	28.48	28.49	27.54	27.56	27.56	26.68	26.69
Texture1	MSSIM	0.9764	0.9758	0.9764	0.9682	0.9697	0.9700	0.9591	0.9592
	PSNR	34.50	34.55	34.55	32.69	32.79	32.79	31.21	31.27
Texture2	MSSIM	0.8312	0.8308	0.8313	0.8113	0.8107	0.8113	0.7927	0.7928
	PSNR	27.59	27.60	27.61	27.04	27.04	27.05	26.52	26.54

Table 5

Processing time and number of iterations for Bazan model.

Images	Measure	$\sigma^* = 0.01$		
		Existing scheme [15]	Proposed with SOR	Proposed with Hybrid BiCGSatb
Lena	Time (s)	128.9474	136.1605	30.0455
	Iterations	121	75	43
Barb	Time (s)	89.5359	95.8069	17.9623
	Iterations	112	69	40
Cameraman	Time (s)	143.2059	151.2620	42.6637
	Iterations	132	83	58
Einstein	Time (s)	155.3026	168.2245	38.1891
	Iterations	149	91	56

Table 6

MSSIM and PSNR for fixed number of iterations for Bazan model.

Images	Measure	$\sigma^* = 0.01$ (40 Iterations)			$\sigma^* = 0.02$ (60 Iterations)		
		Existing scheme [15]	Proposed with SOR	Proposed with Hybrid BiCGSatb	Existing scheme [15]	Proposed with SOR	Proposed with Hybrid BiCGSatb
Lena	MSSIM	0.6210	0.7726	0.8279	0.5166	0.7474	0.7725
	PSNR	25.21	27.38	28.32	22.68	26.02	26.51
Barb	MSSIM	0.6776	0.7427	0.7475	0.5548	0.6822	0.6903
	PSNR	24.52	25.70	25.96	21.95	24.27	24.56
Cameraman	MSSIM	0.6297	0.7685	0.8022	0.6492	0.7577	0.7585
	PSNR	25.34	26.95	27.32	24.11	25.65	25.58
Einstein	MSSIM	0.5519	0.6848	0.7191	0.4439	0.6128	0.6646
	PSNR	25.44	27.77	28.69	22.82	25.65	27.01

to C-model, we show in Figs. 23–24 the denoising for a fixed number of iterations across all the methods for Bazan model. The proposed method performs well in comparison to the existing methods as shown in Figs. 25–26 in terms of MSSIM and PSNR values respectively. This is also verified quantitatively in Table 6. Hence, from above discussion and the comparison of the visual and quantity measures, we can state that the hybrid BiCGStab method for denoising is clearly a favorable option so as to balance the trade-off between the denoising efficacy and computational efficiency.

6. Conclusion

In this paper, we compared two different iterative solvers, namely SOR and Hybrid BiCGStab, for the Crank–Nicolson numerical scheme to solve image denoising problem using C-model and Bazan model. We claimed robustness of the proposed denoising strategy using various images along different levels of noise. It has been found that hybrid BiCGStab solver is capable of solving the model more efficiently than SOR as demonstrated by the higher values of PSNR and MSSIM, in the examples discussed. In this context it is worth mentioning that the C–N scheme, with both of these solvers, produces better PSNR and MSSIM values than the existing method in most of the cases. In addition it has low computational cost due to less number of iterations.

In future, our main focus will be to extend this work to solve the model equation using higher order accurate finite difference schemes with advanced iterative solver.

References

- [1] R.C. Gonzalez, R.E. Woods, *Digital Image Processing*, 2002.
- [2] J. Nolen, *Partial differential equations and diffusion processes*, Tech. Rep., Technical Report, Stanford University. Department of Mathematics, 2009.
- [3] A. Buades, B. Coll, J.M. Morel, On image denoising methods, CMLA Preprint 5.
- [4] J. Weickert, *Anisotropic Diffusion in Image Processing*, Vol. 1, Teubner Stuttgart, 1998.
- [5] A.P. Witkin, Scale-space filtering: A new approach to multi-scale description, in: *Acoustics, Speech, and Signal Processing, IEEE International Conference on ICASSP'84.*, Vol. 9, IEEE, 1984, pp. 150–153.
- [6] P. Perona, J. Malik, Scale-space and edge detection using anisotropic diffusion, *IEEE Trans. Pattern Anal. Mach. Intell.* 12 (7) (1990) 629–639.
- [7] M. Nitzberg, T. Shiota, Nonlinear image filtering with edge and corner enhancement, *IEEE Trans. Pattern Anal. Mach. Intell.* 14 (8) (1992) 826–833.
- [8] J. Weickert, A review of nonlinear diffusion filtering, in: *Scale-Space Theory in Computer Vision*, Springer, 1997, pp. 1–28.
- [9] S. Kichenassamy, The perona–malik paradox, *SIAM J. Appl. Math.* 57 (5) (1997) 1328–1342.
- [10] F. Catté, P.-L. Lions, J.-M. Morel, T. Coll, Image selective smoothing and edge detection by nonlinear diffusion, *SIAM J. Numer. Anal.* 29 (1) (1992) 182–193.
- [11] C. Tomasi, R. Manduchi, Bilateral filtering for gray and color images, in: *Computer Vision, 1998. Sixth International Conference on*, IEEE, 1998, pp. 839–846.
- [12] S. Paris, F. Durand, A fast approximation of the bilateral filter using a signal processing approach, in: *Computer Vision–ECCV 2006*, Springer, 2006, pp. 568–580.

- [13] A. Sameh Arif, S. Mansor, R. Logeswaran, Combined bilateral and anisotropic-diffusion filters for medical image de-noising, in: Research and Development (SCOReD), 2011 IEEE Student Conference on, IEEE, 2011, pp. 420–424.
- [14] M.H. Zeinali, S. Saryazdi, H.K. Rafsanjani, Image denoising via combination anisotropic diffusion and bilateral filtering, in: Computational Intelligence and Communication Networks, CICN, 2011 International Conference on, IEEE, 2011, pp. 421–425.
- [15] C. Bazan, P. Blomgren, Image smoothing and edge detection by nonlinear diffusion and bilateral filter, in: CSRCR2007 21, 2007, pp. 2–15.
- [16] C. Bazán, M. Miller, P. Blomgren, Structure enhancement diffusion and contour extraction for electron tomography of mitochondria, *J. Struct. Biol.* 166 (2) (2009) 144–155.
- [17] M. Gh, C. Bazan, G. Frey, oolume se spatio esholdin xtraction.
- [18] D. Barash, Fundamental relationship between bilateral filtering, adaptive smoothing, and the nonlinear diffusion equation, *IEEE Trans. Pattern Anal. Mach. Intell.* 24 (6) (2002) 844–847.
- [19] J.W. Thomas, Numerical Partial Differential Equations: Finite Difference Methods, Vol. 22, Springer, 1995.
- [20] J. Crank, P. Nicolson, A practical method for numerical evaluation of solutions of partial differential equations of the heat-conduction type, *Adv. Comput. Math.* 6 (3) (1996) 207–226.
- [21] Y. Saad, Iterative Methods for Sparse Linear Systems, second edition, SIAM, Philadelphia, Pennsylvania, 2003.
- [22] G.L. Sleijpen, H.A. Van der Vorst, Hybrid bi-conjugate gradient methods for CFD problems, in: Computational Fluid Dynamics Review 1995, 1995, pp. 457–476.
- [23] J. Weickert, B.T.H. Romeny, M.A. Viergever, Efficient and reliable schemes for nonlinear diffusion filtering, *IEEE Trans. Image Process.* 7 (3) (1998) 398–410.
- [24] K.W. Morton, Numerical Solution of Partial Differential Equations: An Introduction, Cambridge university press, 2005.
- [25] W. Wang, Y. Shi, An image denoising algorithm in the matrix form, in: Multimedia Technology (ICMT), 2011 International Conference on, IEEE, 2011, pp. 176–179.
- [26] Y. Shi, Y. Zhu, J. Liu, Semi-implicit image denoising algorithm for different boundary conditions, *TELKOMNIKA Indones. J. Electr. Eng.* 11 (4) (2013) 2058–2063.
- [27] G.H. Golub, C.F. Van Loan, Matrix Computations, Vol. 3, JHU Press, 2012.
- [28] A. Greenbaum, Iterative Methods for Solving Linear Systems, Vol. 17, SIAM, 1997.
- [29] J.R. Shewchuk, An introduction to the conjugate gradient method without the agonizing pain, 1994.
- [30] P. Sonneveld, CGS, a fast lanczos-type solver for nonsymmetric linear systems, *SIAM J. Sci. Stat. Comput.* 10 (1) (1989) 36–52.
- [31] R. Fletcher, Conjugate gradient methods for indefinite systems, in: Numerical Analysis, Springer, 1976, pp. 73–89.
- [32] G.L. Sleijpen, D.R. Fokkema, BiCGstab (l) for linear equations involving unsymmetric matrices with complex spectrum, *Electron. Trans. Numer. Anal.* 1 (11) (1993) 2000.
- [33] Y. Saad, M.H. Schultz, GMRES: A generalized minimal residual algorithm for solving nonsymmetric linear systems, *SIAM J. Sci. Stat. Comput.* 7 (3) (1986) 856–869.
- [34] S. Sickel, M.-C. Yeung, M.J. Held, A comparison of some iterative methods in scientific computing, Summer Reserch Apprentice Program.
- [35] P. Mrázek, M. Navara, Selection of optimal stopping time for nonlinear diffusion filtering, *Int. J. Comput. Vis.* 52 (2–3) (2003) 189–203.
- [36] J. Weickert, Coherence-enhancing diffusion of colour images, *Image Vis. Comput.* 17 (3) (1999) 201–212.
- [37] I.C. Dolcetta, R. Ferretti, Optimal stopping time formulation of adaptive image filtering, *Appl. Math. Optim.* 43 (3) (2001) 245–258.
- [38] V. Solo, Automatic stopping criterion for anisotropic diffusion, in: ICASSP, Vol. 1, Citeseer, 2001, pp. 3441–3444.
- [39] V. Solo, A fast automatic stopping criterion for anisotropic diffusion, in: Acoustics, Speech, and Signal Processing (ICASSP), 2002 IEEE International Conference on, Vol. 2, IEEE, 2002, pp. 1661–1664.
- [40] G. Gilboa, N. Sochen, Y.Y. Zeevi, Estimation of optimal PDE-based denoising in the SNR sense, *IEEE Trans. Image Process.* 15 (8) (2006) 2269–2280.
- [41] G. Gilboa, Nonlinear scale space with spatially varying stopping time, *IEEE Trans. Pattern Anal. Mach. Intell.* 30 (12) (2008) 2175–2187.
- [42] A. Ilyevsky, E. Turkel, Stopping criteria for anisotropic PDEs in image processing, *J. Sci. Comput.* 45 (1–3) (2010) 333–347.
- [43] Z. Wang, A.C. Bovik, H.R. Sheikh, E.P. Simoncelli, Image quality assessment: from error visibility to structural similarity, *IEEE Trans. Image Process.* 13 (4) (2004) 600–612.
- [44] Z. Wang, A.C. Bovik, Mean squared error: love it or leave it? A new look at signal fidelity measures, *IEEE Signal Process. Mag.* 26 (1) (2009) 98–117.